Anomalous Conductance Oscillations in the Hybridization Gap of InAs/GaSb Quantum Wells

Zhongdong Han, Tingxin Li, Long Zhang, Gerard Sullivan, and Rui-Rui Du

Phys. Rev. Lett. **123**, 126803 — Published 20 September 2019

DOI: 10.1103/PhysRevLett.123.126803

Anomalous Conductance Oscillations in the Hybridization Gap of InAs/GaSb Quantum Wells

Zhongdong Han[1], Tingxin Li[2], Long Zhang[3,*], Gerard Sullivan[5] and Rui-Rui Du[1,2,4,†]

[1]*International Center for Quantum Materials, School of Physics, Peking University, Beijing 100871, China*
[2]*Department of Physics and Astronomy, Rice University, Houston, Texas 77251-1892, USA*
[3]*Kavli Institute for Theoretical Sciences and CAS Center for Excellence, University of Chinese Academy of Sciences, Beijing 100190, China*
[4]*Collaborative Innovation Center of Quantum Matter, Beijing 100871, China*
[5]*Teledyne Scientific and Imaging, Thousand Oaks, California 91603, USA*

[*]Long Zhang: longzhang@ucas.ac.cn; [†]Rui-Rui Du: rrd@rice.edu

Abstract

We observe the magnetic oscillation of electric conductance in the two-dimensional InAs/GaSb quantum spin Hall insulator. Its insulating bulk origin is unambiguously demonstrated by the antiphase oscillations of the conductance and the resistance. Characteristically, the in-gap oscillation frequency is higher than the Shubnikov-de Haas oscillation close to the conduction band edge in the metallic regime. The temperature dependence shows both thermal activation and smearing effects, which cannot be described by the Lifshitz-Kosevich theory. A two-band Bernevig-Hughes-Zhang model with a large quasiparticle self-energy in the insulating regime is proposed to capture the main properties of the in-gap oscillations.

Introduction.- Magnetic oscillations in metals stem from the Landau quantization of charged particles in magnetic field, and have been a standard tool to measure the Fermi surfaces of metals [1]. In two-dimensional electron systems (2DES), the Shubnikov-de Haas (SdH) oscillation of conductance evolves into the integer quantum Hall effect when only a few Landau levels (LLs) are filled. In the fractional quantum Hall effect, the magnetic oscillations of composite fermions offer a unique window looking into many-body physics in this strongly interacting electron system [2,3].

Recently, unconventional magnetization and resistivity oscillations were observed in the Kondo insulators, SmB_6 and YbB_{12} [4-8], which challenged the canonical theory of magnetic oscillations and triggered intense studies and controversies. The first concern is whether these oscillations come from the insulating bulk states. This is obscured by the presence of metallic surface states in the 3D topological Kondo insulators [4,9,10]. Therefore, it is particularly desirable to observe magnetic oscillations in 2D topological insulators, e.g., the InAs/GaSb quantum well (QW) [11], in which the bulk and edge transport channels can be clearly distinguished by designing different sample geometries. This is achieved in this work, and the insulating bulk state is shown to be the origin of the in-gap conductance oscillations.

Second, it is not clear whether the in-gap oscillations can be captured by the Landau quantization of gapped single-particle states [12-15] or whether one must consider some kind of (nearly) gapless charge-neutral excitations [16-20]. In experiments, the absence of low-temperature thermal conductivity [21,22] (cf. Refs. [6,23]) poses a severe constraint on charge-neutral excitations. On the other hand, in single-particle models,

the in-gap oscillations require a narrow hybridization gap [12-14]. The electron interactions and disorders can introduce a finite quasiparticle self-energy and reduce the hybridization gap, thereby significantly enhance the in-gap oscillations [15,23].

In this work, we report the observation of magnetic oscillations in the 2D InAs/GaSb quantum spin Hall (QSH) insulator. The magnetic oscillations are observed both in the resistance of a Hall bar and in the conductance of a Corbino disk device. They exhibit a π phase difference. This demonstrates the insulating bulk origin of the in-gap oscillations. The in-gap oscillation frequency is higher than the SdH oscillation in the conduction band close to the band edge. This is captured by a two-band Bernevig-Hughes-Zhang model with a large quasiparticle self-energy introduced phenomenologically in the insulating regime, which may be attributed to the unscreened Coulomb interaction. The temperature dependence of the in-gap oscillation strongly deviates from the conventional Lifshitz-Kosevich (LK) theory in metals [1,24]. The oscillation amplitude can either increase (thermal activation) or decrease (thermal smearing) with the temperature depending on the Fermi energy, which is qualitatively consistent with the theoretical predictions in narrow-gap topological insulators [11,13].

Materials and methods.- The InAs/GaSb QW is a type-II semiconductor heterostructure. The valence band edge of the GaSb layer is higher than the conduction band edge of the InAs layer. The hybridization of these spatially separated electron and hole bands opens a mini-gap [25]. It has been established to be a highly tunable platform to realize the 2D QSH effect [26-28].

The InAs/GaSb QWs are grown on the n-type GaSb substrate by molecular beam

epitaxy. The detailed structure of the QW is shown in the Supplemental Materials. Both dual-gated Hall bars and Corbino disk devices are fabricated. Except for the R_{xx} trace in Fig. 2a, all conductance oscillations are measured from a Corbino device. The measurements are performed using the standard low-frequency lock-in technique in a ^{3}He cryostat equipped with a superconducting magnet coil up to 9 T. We also measure the conductance in tilted magnetic field in a ^{3}He cryostat equipped with a superconducting magnet up to 15 T. All data are taken at 300 mK except for the temperature dependence measurements.

We also fabricate the strained-layer InAs/$Ga_{0.68}In_{0.32}Sb$ QSH insulator, which has a larger hybridization gap and a more insulating bulk state [29,30]. Similar in-gap resistance oscillations are observed and described in detail in the Supplemental Materials.

In-gap magnetic oscillations from insulating bulk state.- We first show a standard Landau fan diagram to visualize the LLs of the InAs/GaSb QW in a perpendicular magnetic field $B_\perp$. A 2D map of the conductance G_{xx} measured with a Corbino device as a function of the front gate bias V_f and $B_\perp$ is shown in Fig. 1a. The gating V_f tunes the Fermi energy from the conduction band to the valence band across the hybridization gap. One representative G_{xx} curve in each regime is drawn in Fig. 1c. The blue and the red curves exhibit typical SdH oscillations of 2D metals. Surprisingly, the conductance oscillation is also observed in the QSH insulator regime (black curve). While the Landau level spectra in inverted InAs/GaSb system have been reported in a number of interesting experimental papers [31-33], the present work will focus on the

in-gap magnetic oscillations.

Does the in-gap conductance oscillation come from the insulating bulk state? This is a major issue not fully settled in 3D Kondo insulators due to the presence of metallic surface states [4,9,10]. Fortunately, the electric transport of the bulk and the edge states can be distinguished in 2D devices of the InAs/GaSb QWs. The conductance G_{xx} and the resistance R_{xx} are measured with a Corbino disk and a Hall bar device, respectively. They show antiphase oscillations with $B_\perp$ (Fig. 2a).

First, in the Corbino device, the edge states are shunted by the metal electrodes, thus the conductance is only contributed by the bulk state. Second, the bulk resistance reaches $200\ \mathrm{k\Omega}$ at zero magnetic field, which is order-of-magnitude larger than the resistance quantum $h/e^2 = 25.8\ \mathrm{k\Omega}$, and thus the bulk state is sufficiently insulating. In 2D metals, the Hall resistivity ρ_{xy} is much larger than the longitudinal resistivity ρ_{xx} in a moderate $B_\perp$, thus the conductivity $\sigma_{xx} = \rho_{xx}/(\rho_{xx}^2 + \rho_{xy}^2) \simeq \rho_{xx}/\rho_{xy}^2 \propto \rho_{xx}$ should show in-phase oscillations as ρ_{xx}. However, in an insulator, $\rho_{xy} \ll \rho_{xx}$, thus $\sigma_{xx} \simeq 1/\rho_{xx}$, leading to the antiphase oscillations of G_{xx} and R_{xx}. Therefore, the above observations unambiguously demonstrate that the in-gap magnetic oscillations originate from the insulating bulk state.

The in-gap conductance oscillation is approximately periodic in $1/B$ like the SdH effect in metals. In single-particle models of magnetic oscillations in hybridized insulators, the oscillation frequency is determined by the electron density n_0 of the compensated semimetal if the band hybridization is turned off [12-15,23],

$$\frac{\Delta\nu}{\Delta(1/B)} = \frac{h}{e} n_0, \qquad (1)$$

in which ν is the filling factor. We plot the filling factor diagram of the conductance minima in Fig. 2b. The fitting yields $n_0 = (1.63 \pm 0.05) \times 10^{11}$ cm^{-2}. Quite unexpectedly, the electron density n exhibits a jump when V_f is tuned from the conduction band into the hybridization gap (Fig. 2b, inset). In other words, the electron density in the conduction band extracted from the SdH oscillations can be smaller than n_0.

The InAs/GaSb QSH insulator is described by the two-band Bernevig-Hughes-Zhang (BHZ) model [26,34],

$$H_0 = \begin{pmatrix} h(k) & 0 \\ 0 & h^*(-k) \end{pmatrix},$$

$$h(k) = \begin{pmatrix} \frac{\hbar^2 k^2}{2m_e^*} - \mu_e & w(k_x + ik_y) \\ w(k_x - ik_y) & -\frac{\hbar^2 k^2}{2m_h^*} + \mu_h \end{pmatrix}.$$

Here, the electron and hole effective masses $m_e^* = 0.040m_e$ and $m_h^* = 0.136m_e$ are taken in accord with the experiments [35]. The band inversion $\mu_e + \mu_h = \pi\hbar^2 n_0(1/m_e^* + 1/m_h^*)$. We set $w = 0.8$ eV · Å, which is comparable to the results of first-principle calculations with similar QW widths [36].

The band structure of the BHZ model is shown in Fig. 2c. When the Fermi energy is in the conduction band, the SdH oscillation frequency is proportional to the electron density n_e, $\frac{\Delta\nu}{\Delta(1/B)} = \frac{h}{e}n_e$, which vanishes as the Fermi energy decreases to the band bottom.

In 2DES, the Coulomb interactions lead to a finite quasiparticle self-energy Σ, which should be quite large in the insulating regime due to the absence of charge screening. Here we treat $\Sigma = \mathrm{diag}\,(-i\Gamma_e, -i\Gamma_h, -i\Gamma_e, -i\Gamma_h)$ as phenomenological

parameters, and consider the asymmetric case $\Gamma_h > \Gamma_e$ because of the larger hole mass. As shown by H. Shen and L. Fu [15], the asymmetric self-energy reduces the hybridization gap (see Fig. 2c) and greatly enhances the in-gap oscillation, and the frequency is given by Eq. (1). Therefore, the oscillation frequency exhibits a jump compared to the SdH frequency in the metallic regime as a consequence of the enhanced self-energies in the insulating regime.

The density of states (DOS) at the Fermi energy in magnetic field are calculated in both the metallic and the insulating regimes assuming different self-energies, $D(\epsilon) = 2\mathrm{Im}\mathrm{Tr}(H_0 + \Sigma - \epsilon)^{-1}$, and the details are shown in the Supplemental Materials. The calculated carrier density n is found to exhibit the similar variation as the experiments (Fig. 2d). We note that such a variation cannot be produced if the self-energy is taken to be the same in both regimes (see the Supplemental Materials). Therefore, this peculiar variation of the frequency points to the strong Coulomb interaction effect particularly in the insulating regime.

The band inversion of the QW can be tuned by the back gate V_b when fixing the chemical potential inside the gap by changing V_f. The evolution of the in-gap conductance is shown in Fig. 4a. As V_b is tuned from $3\,\mathrm{V}$ to $-1\,\mathrm{V}$, the band inversion gradually decreases and all oscillatory features shift to lower $B_\perp$, thus the oscillation frequency is reduced. This is consistent with Eq. (1) from the two-band model.

Temperature dependence.- The temperature dependence of the in-gap conductance is shown in Fig. 3. In order to extract the oscillation amplitudes, we take the second-

order derivative $-\partial_{B^{-1}}^2 G_{xx}$ to remove the monotonic background, which is shown in Figs. 3b and 3c. As the temperature increases, the in-gap oscillation amplitude near the valence band edge ($V_f = -0.85$ V) gradually decreases (Fig. 3b), which is reminiscent of the LK theory of thermal smearing effect in metals [1,24]. However, at the charge neutral point (CNP) ($V_f = -0.75$ V), the oscillation amplitude increases with the temperature (Fig. 3c), suggesting a thermal activation behavior, which cannot be described by the LK theory. Therefore, the temperature effect on the in-gap oscillations is two-fold, thermal smearing and activation, which is qualitatively consistent with the theory of DOS oscillations of in narrow-gap insulators [11,13].

Robustness to in-plane magnetic field.- Applying an in-plane magnetic field $B_{\parallel}$ on type-II semiconductor QWs is supposed to induce a relative momentum shift between the electron and the hole bands, $\Delta k = eB_{\parallel}\langle z\rangle/\hbar$, in which $\langle z\rangle$ is the vertical distance of the electron and the hole layers. This may close the hybridization gap [25]. However, we find that the in-plane magnetic field (up to 12T) has weak effect on the in-gap oscillations in the sample studied (Fig. 4b).

The robustness against $B_{\parallel}$ may be understood by considering the effect of the interband Coulomb interaction. It can reduce the spatial separation $\langle z\rangle$ of electrons and holes and the momentum shift Δk, thus making the hybridization gap more robust against $B_{\parallel}$. Moreover, it can bind the electrons and holes into excitons, leading to a topological excitonic insulator (TEI) state [37,38]. In experiments, the TEI state is found in InAs/GaSb QWs with $n_0 < 1 \times 10^{11}$ cm^{-2} [39], and the exciton gap is remarkably robust against $B_{\parallel}$. However, in Ref. [39], n_0 was estimated by linearly

extrapolating n in the conduction band to the CNP, which may underestimate n_0 according to our current analysis. In our devices, $n_0 = (1.63 \pm 0.05) \times 10^{11}$ cm^{-2}, thus the TEI state may also set in and reinforce the robustness against $B_{\parallel}$.

Summary and discussion.- In summary, the magnetic oscillation of conductance is observed in the hybridization gap of inverted InAs/GaSb QWs. The antiphase oscillations of the conductance and the resistance demonstrate their insulating bulk origin. The variation of the oscillation frequency with the front gate bias V_f can be captured by a two-band BHZ model with the phenomenological assumption of a large quasiparticle self-energy in the insulating regime, which may be attributed to the strong Coulomb interaction. The temperature dependence of the in-gap oscillation amplitudes shows both thermal smearing and thermal activation behaviors, which strongly deviates from the conventional LK theory. The in-plane magnetic field has rather weak effect on the in-gap oscillations.

In a recent preprint by D. Xiao et al [40], the in-gap resistance oscillation in a wider InAs/GaSb QW was also reported; the InAs/GaSb QW width is 15 nm/10 nm. An oscillation frequency jump was also found when the gate voltage tunes the Fermi energy from the conduction band to the hybridization gap. Their measurements were only performed on Hall-bar devices, and the electron density at the CNP is $n_0 \simeq 2 \times 10^{12}$ cm^{-2}, much larger than our sample.

Acknowledgements

We gratefully acknowledge C. L. Yang and P. L. Li for the assistance in titled magnetic field experiments. This work is supported by National Key R&D Program of China (No.

2017YFA0303301 and No. 2018YFA0305800), Strategic Priority Research Program of Chinese Academy of Sciences (No. XDB28000000), National Natural Science Foundation of China (No. 11804337), and Beijing Municipal Science & Technology Commission (No. Z181100004218001). Work at Rice University is supported by NSF Grant No. DMR-1508644 and Welch Foundation Grant No. C-1682.

References

[1] D. Shoenberg, *Magnetic Oscillations in Metals* (Cambridge University Press, Cambridge, 1984).

[2] B. I. Halperin, P. A. Lee, and N. Read, Phys. Rev. B 47, 7312(1993).

[3] J. K. Jain, *Composite Fermions* (Cambridge University Press, Cambridge, 2007).

[4] G. Li, Z. Xiang, F. Yu, T. Asaba, B. Lawson, P. Cai, C. Tinsman, A. Berkley, S. Wolgast, Y. S. Eo, D.-J. Kim, C. Kurdak, J. W. Allen, K. Sun, X. H. Chen, Y. Y. Wang, Z. Fisk, and L. Li, Science 346, 1208 (2014).

[5] B. S. Tan, Y.-T. Hsu, B. Zeng, M. C. Hatnean, N. Harrison, Z. Zhu, M. Hartstein, M. Kiourlappou, A. Srivastava, M. D. Johannes, T. P. Murphy, J.-H. Park, L. Balicas, G. G. Lonzarich, G. Balakrishnan, and S. E. Sebastian, Science 349, 287 (2015).

[6] M. Hartstein, W. H. Toews, Y.-T. Hsu, B. Zeng, X. Chen, M. C. Hatnean, Q. R. Zhang, S. Nakamura, A. S. Padgett, G. Rodway-Gant, J. Berk, M. K. Kingston, G. H. Zhang, M. K. Chan, S. Yamashita, T. Sakakibara, Y. Takano, J.-H. Park, L. Balicas, N. Harrison, N. Shitsevalova, G. Balakrishnan, G. G. Lonzarich, R. W. Hill, M. Sutherland, and S. E. Sebastian, Nat. Phys. 14, 166 (2018).

[7] H. Liu, M. Hartstein, G. J. Wallace, A. J. Davies, M. C. Hatnean, M. D. Johannes,

N. Shitsevalova, G. Balakrishnan, and S. E. Sebastian, J. Phys. Condens. Matter 30, 16LT01 (2018).

[8] Z. Xiang, Y. Kasahara, T. Asaba, B. Lawson, C. Tinsman, L. Chen, K. Sugimoto, S. Kawaguchi, Y. Sato, G. Li, S. Yao, Y. L. Chen, F. Iga, J. Singleton, Y. Matsuda, and L. Li, Science 362, 65 (2018).

[9] O. Erten, P. Ghaemi, and P. Coleman, Phys. Rev. Lett. 116, 046403 (2016).

[10] J. D. Denlinger, S. Jang, G. Li, L. Chen, B. J. Lawson, T. Asaba, C. Tinsman, F. Yu, K. Sun, J. W. Allen, C. Kurdak, D.-J. Kim, Z. Fisk, and L. Li, arXiv:1601.07408.

[11] J. Knolle and N. R. Cooper, Phys. Rev. Lett. 118, 176801 (2017).

[12] J. Knolle and N. R. Cooper, Phys. Rev. Lett. 115, 146401 (2015).

[13] L. Zhang, X.-Y. Song, and F. Wang, Phys. Rev. Lett. 116, 046404 (2016).

[14] H. K. Pal, F. Piéchon, J.-N. Fuchs, M. Goerbig, and G. Montambaux, Phys. Rev. B 94, 125140 (2016).

[15] H. Shen and L. Fu, Phys. Rev. Lett. 121, 026403 (2018).

[16] G. Baskaran, arXiv:1507.03477.

[17] J. Knolle and N. R. Cooper, Phys. Rev. Lett. 118, 096604 (2017).

[18] O. Erten, P.-Y. Chang, P. Coleman, and A. M. Tsvelik, Phys. Rev. Lett. 119, 057603 (2017).

[19] D. Chowdhury, I. Sodemann, and T. Senthil, Nat. Commun. 9, 1766 (2018).

[20] I. Sodemann, D. Chowdhury, and T. Senthil, Phys. Rev. B 97, 045152 (2018).

[21] Y. Xu, S. Cui, J. K. Dong, D. Zhao, T. Wu, X. H. Chen, K. Sun, H. Yao, and S. Y. Li, Phys. Rev. Lett. 116, 246403 (2016).

[22] M.-E. Boulanger, F. Laliberté, M. Dion, S. Badoux, N. Doiron-Leyraud, W. A. Phelan, S. M. Koohpayeh, W. T. Fuhrman, J. R. Chamorro, T. M. McQueen, X. F. Wang, Y. Nakajima, T. Metz, J. Paglione, and L. Taillefer, Phys. Rev. B 97, 245141 (2018).

[23] N. Harrison, Phys. Rev. Lett. 121, 026602 (2018).

[24] I. M. Lifshitz and A. M. Kosevich, Sov. Phys. JETP 2, 636 (1956).

[25] M. J. Yang, C. H. Yang, B. R. Bennett, and B. V. Shanabrook, Phys. Rev. Lett. 78, 4613 (1997).

[26] C. Liu, T. L. Hughes, X.-L. Qi, K. Wang, and S.-C. Zhang, Phys. Rev. Lett. 100, 236601 (2008).

[27] I. Knez, R.-R. Du, and G. Sullivan, Phys. Rev. Lett. 107, 136603 (2011).

[28] L. Du, I. Knez, G. Sullivan, and R.-R. Du, Phys. Rev. Lett. 114, 096802 (2015).

[29] L. Du, T. Li, W. Lou, X. Wu, X. Liu, Z. Han, C. Zhang, G. Sullivan, A. Ikhlassi, K. Chang, and R.-R. Du, Phys. Rev. Lett. 119, 056803 (2017).

[30] T. Li, P. Wang, G. Sullivan, X. Lin, and R.-R. Du, Phys. Rev. B 96, 241406(R) (2017).

[31] R. J. Nicholas, K. Takashina, M. Lakrimi, B. Kardynal, S. Khym, N. J. Mason, D. M. Symons, D. K. Maude, and J. C. Portal, Phys. Rev. Lett. 85, 2364 (2000).

[32] K. Suzuki, K. Takashina, S. Miyashita, and Y. Hirayama, Phys. Rev. Lett. 93, 016803 (2004).

[33] Fabrizio Nichele, Atindra Nath Pal, Patrick Pietsch, Thomas Ihn, Klaus Ensslin, Christophe Charpentier, and Werner Wegscheider, Phys. Rev. Lett. 112, 036802 (2014).

[34] B. A. Bernevig, T. L. Hughes, and S.-C. Zhang, Science 314, 1757 (2006).

[35] X. Mu, G. Sullivan, and R.-R. Du, Appl. Phys. Lett. 108, 012101 (2016).

[36] C. Liu and S. Zhang, in *Topological Insulators*, edited by M. Franz and L. Molenkamp (Elsevier, 2013).

[37] Y. Naveh and B. Laikhtman, Phys. Rev. Lett. 77, 900 (1996).

[38] D. I. Pikulin and T. Hyart, Phys. Rev. Lett. 112, 176403 (2014).

[39] L. Du, X. Li, W. Lou, G. Sullivan, K. Chang, J. Kono, and R.-R. Du, Nat. Commun. 8, 1971 (2017).

[40] D. Xiao, C.-X. Liu, N. Samarth, and L.-H. Hu, Phys. Rev. Lett. 122, 186802 (2019).

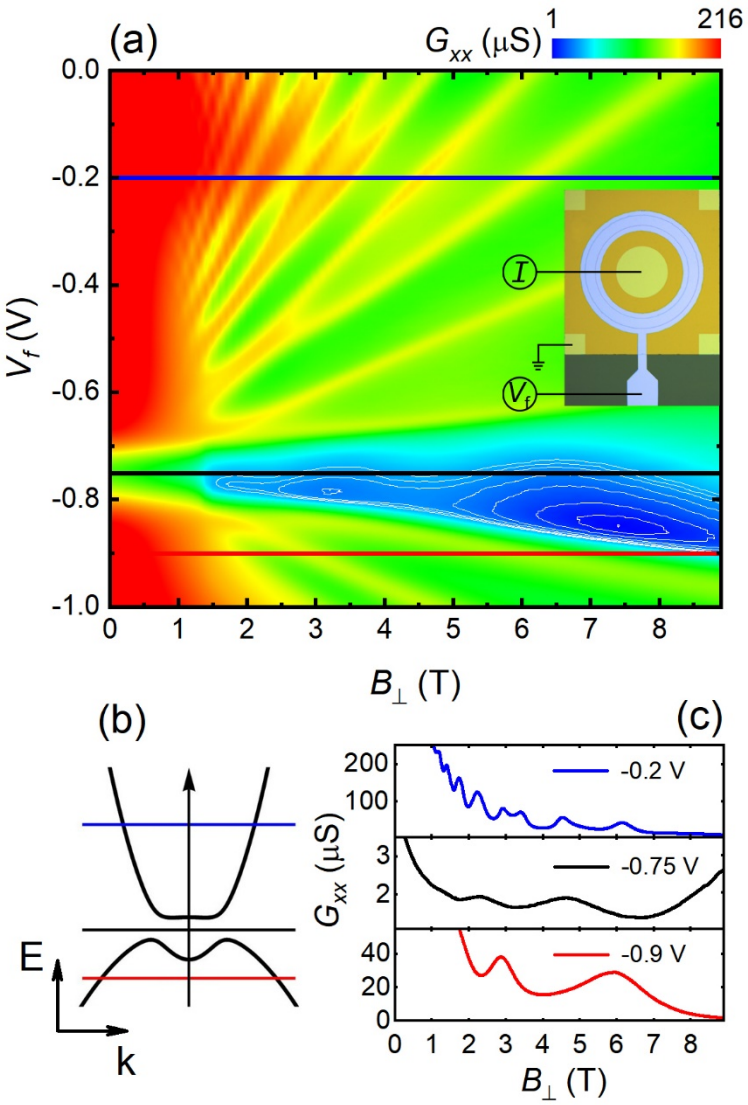

Fig. 1. (a) 2D conductance map as a function of the front gate bias V_f and the perpendicular magnetic field $B_\perp$, which is measured with a Corbino device (optical microscope image in inset) at 300 mK. The conductance traces at three gate biases are plotted in (c) to represent the electron ($V_f = -0.2$ V, blue), the hole ($V_f = -0.9$ V, red) and the insulating ($V_f = -0.75$ V, black) regimes, respectively. The inverted band structure is schematically plotted in (b), where the Fermi energies of the three curves are labeled.

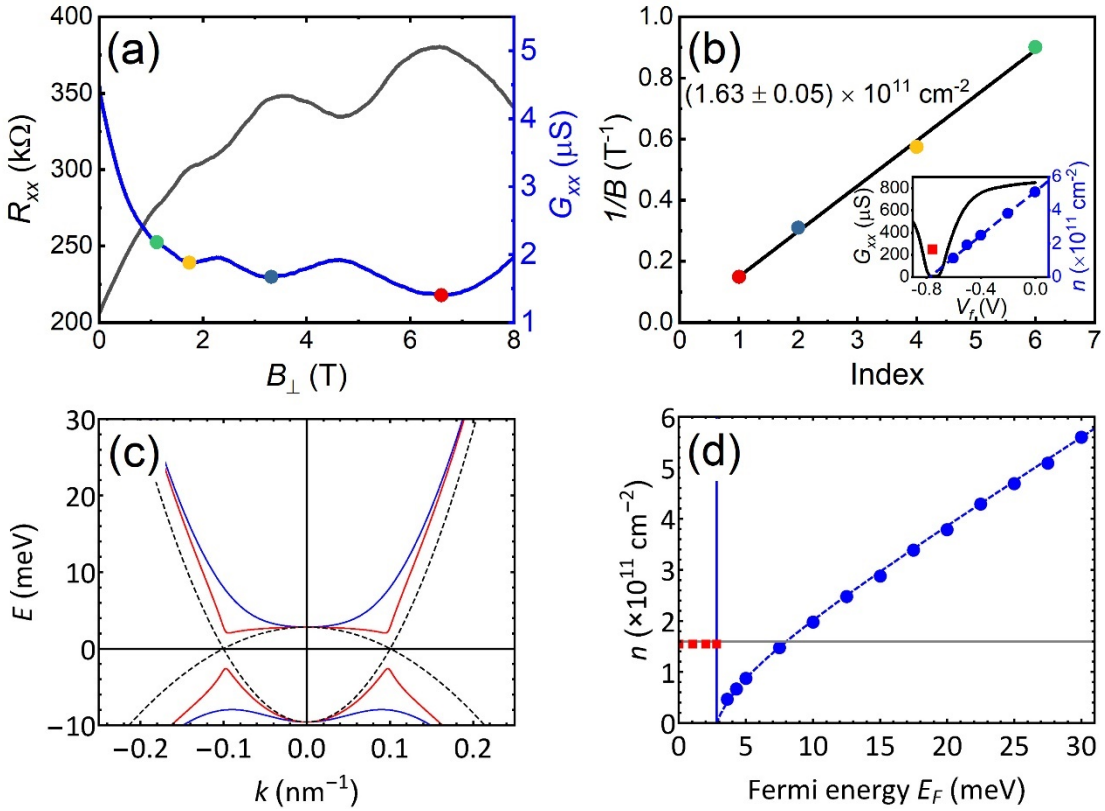

Fig. 2. (a) Anomalous magnetic oscillations of G_{xx} and R_{xx} in the hybridization gap. (b) Filling factor index diagram. The fitting yields $n_0 = (1.63 \pm 0.05) \times 10^{11}$ cm^{-2}. Inset: Electron density n in the conduction band (blue dots) and n_0 in the hybridization gap (red dot), and zero-field conductance G_{xx} (black curve) vs. V_f. The dashed line is guide for the eye. (c) Energy dispersion (real part of the eigenvalues) of $H = H_0 + \Sigma$ with $n_0 = 1.6 \times 10^{11}$ cm^{-2}. Blue lines: $\Gamma_e = \Gamma_h = 0$; red lines: $\Gamma_e = 1$ meV, $\Gamma_h = 16$ meV. Also shown is the dispersion without hybridization (black dashed lines). (d) Electron density fitted from the density of states oscillations calculated from the two-band model. Blue dots: in the metallic regime, $\Gamma_e = 0.2$ meV, $\Gamma_h = 0.4$ meV. Red squares: in the insulating regime, $\Gamma_e = 1$ meV, $\Gamma_h = 16$ meV. n_0 is indicated by the gray line. The blue vertical line indicates the conduction band edge. The dashed line is the Fermi surface area in the conduction band when the self-energy is turned off.

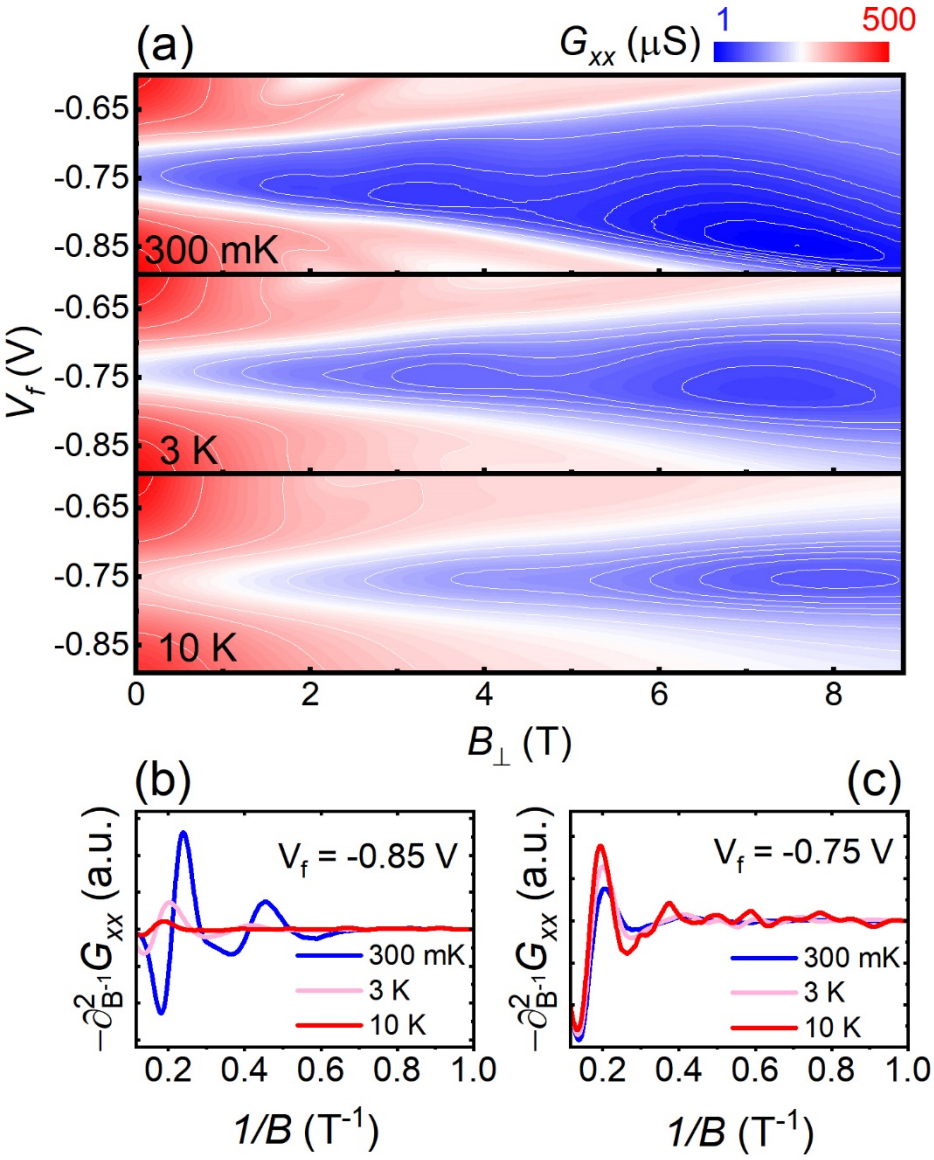

Fig. 3. Temperature dependence of the in-gap oscillations. (a) 2D conductance map in the insulator regime measured at different temperatures. In order to compare the oscillation amplitudes at different temperatures, we remove the background by taking the second-order derivative, $-\partial^2_{B^{-1}} G_{xx}$ in (b) at $V_f = -0.85$ V and (c) at $V_f = -0.75$ V.

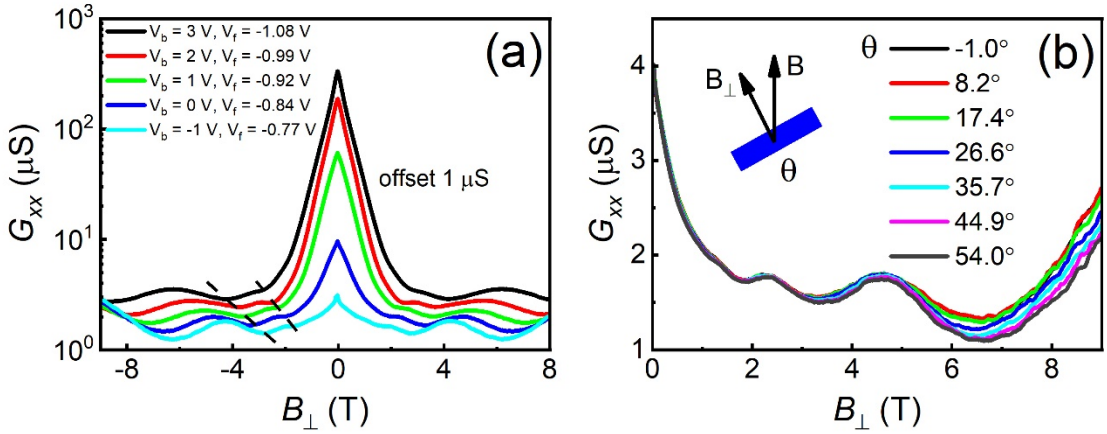

Fig. 4. (a) The in-gap oscillations measured with different back gate biases V_b. The band inversion gradually decreases as V_b is tuned from $3\,\mathrm{V}$ to $-1\,\mathrm{V}$ and simultaneously V_f is adjusted to hold the chemical potential inside the gap. (b) The in-gap oscillations measured in tilted magnetic fields.